하이드로카본 소재 합성 공정 최신전략
Synthetic Strategies of Hydrocarbon Reaction Catalysts/Materials

Uk Sim, Ph. D.

Single Atomic Catalysts

Chem. Eur. J. (2018)
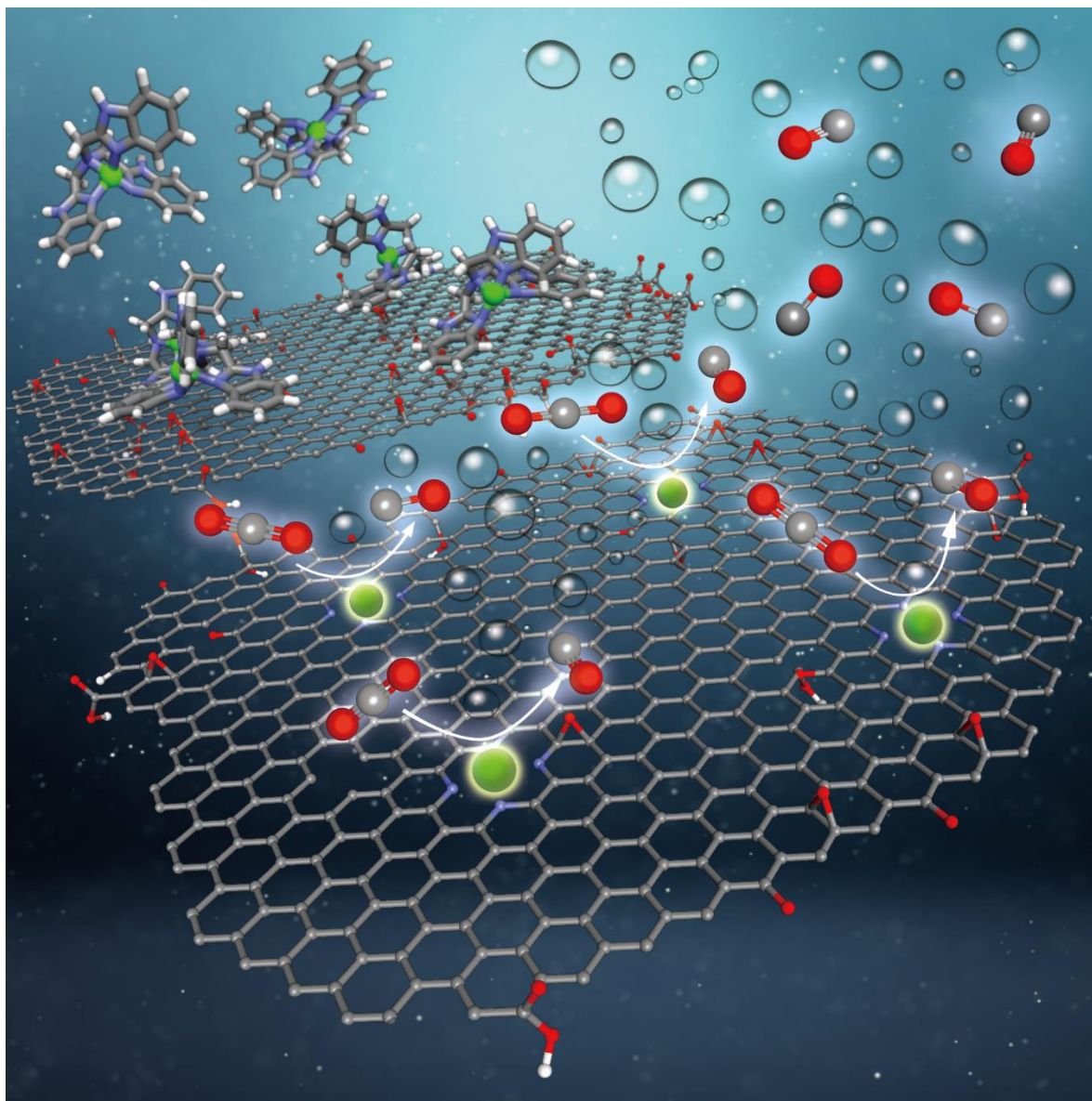
Metal and Nitrogen doped graphene

M-N$_4$ active site over graphene structure
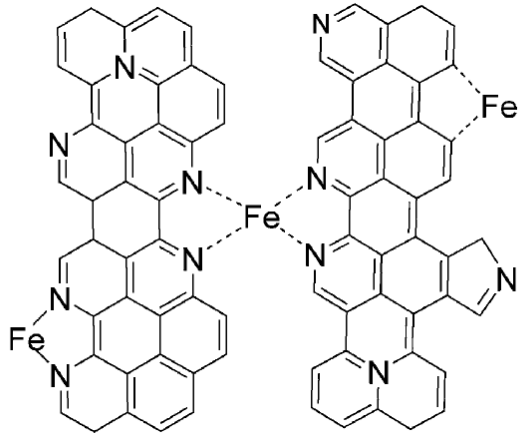
Angew. Chem. Int. Ed. **2015**, 54, 10102 – 10120

Nitrogen doping over graphene

J. Mater. Chem. A, 2016,4, 1144-1173

Metal and nitrogen doping over graphene
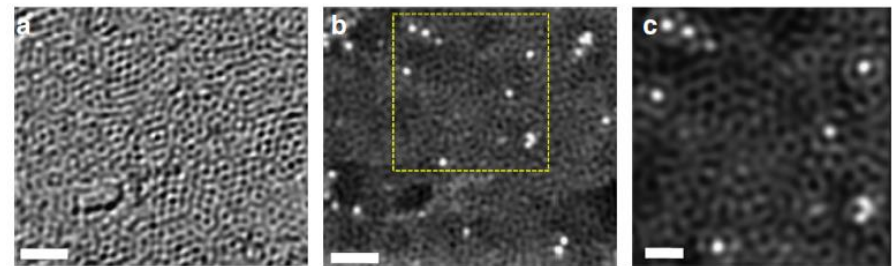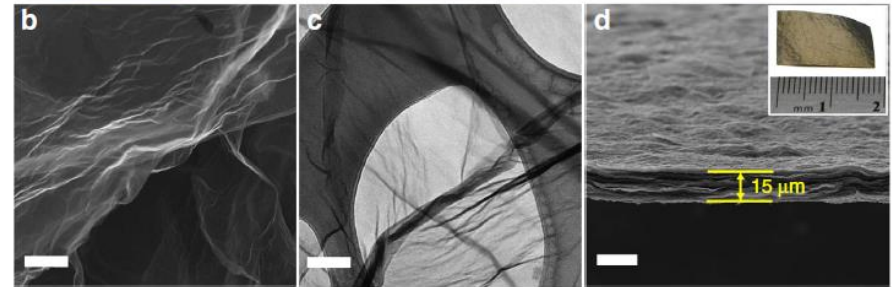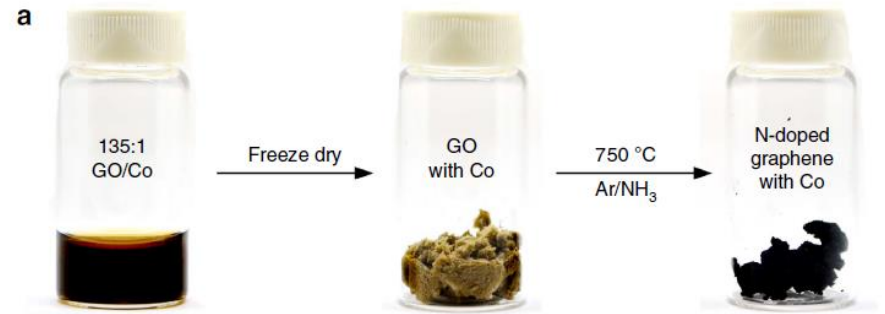
Nature Communications **2015**, 6, Article number: 8668

Ligand assisted metal doping over graphene oxide

Carbonization @ 800°C

Uk Sim et al., Chem. Eur. J. (2018)

Inactive

Metal particle loaded carbon structure

Absorption

Absorption With GO

Annealing @ 800°C

Single Atomic metal over reduced graphene oxide

+ 0.5mg/ml GO

Complex Absorption
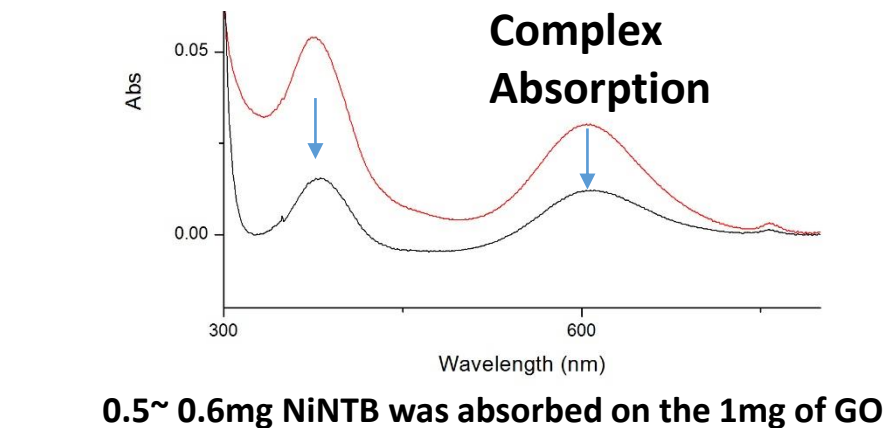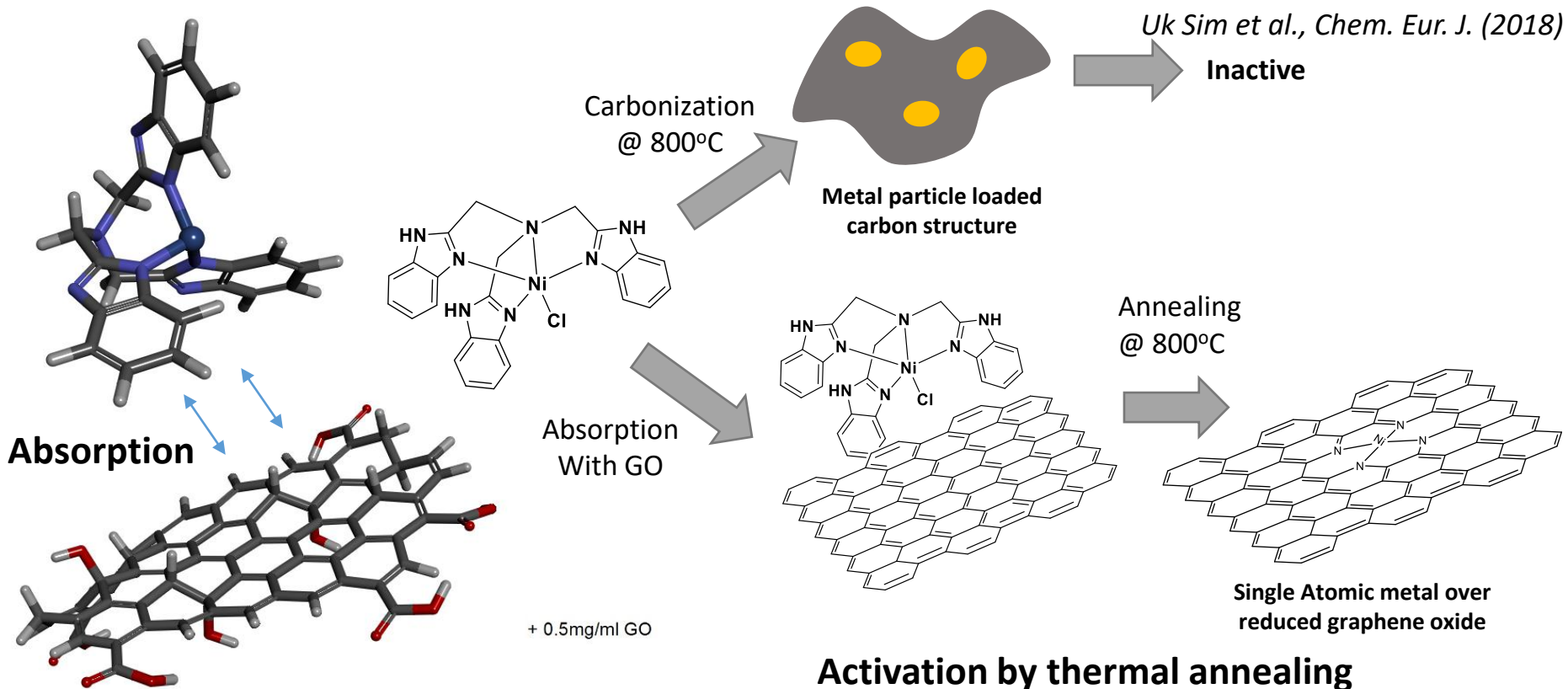
Activation by thermal annealing

Heat Treatment

800°C

0.5~ 0.6mg NiNTB was absorbed on the 1mg of GO

Ni NTB GO

Ni N RGO

Single-Atom Metal Active Sites on Graphene Oxide

Chemical transformation of **nickel tris(2-benzimidazolylmethyl) amine (Ni-NTB)** adsorbed over graphene oxide sheets by the thermal annealing process
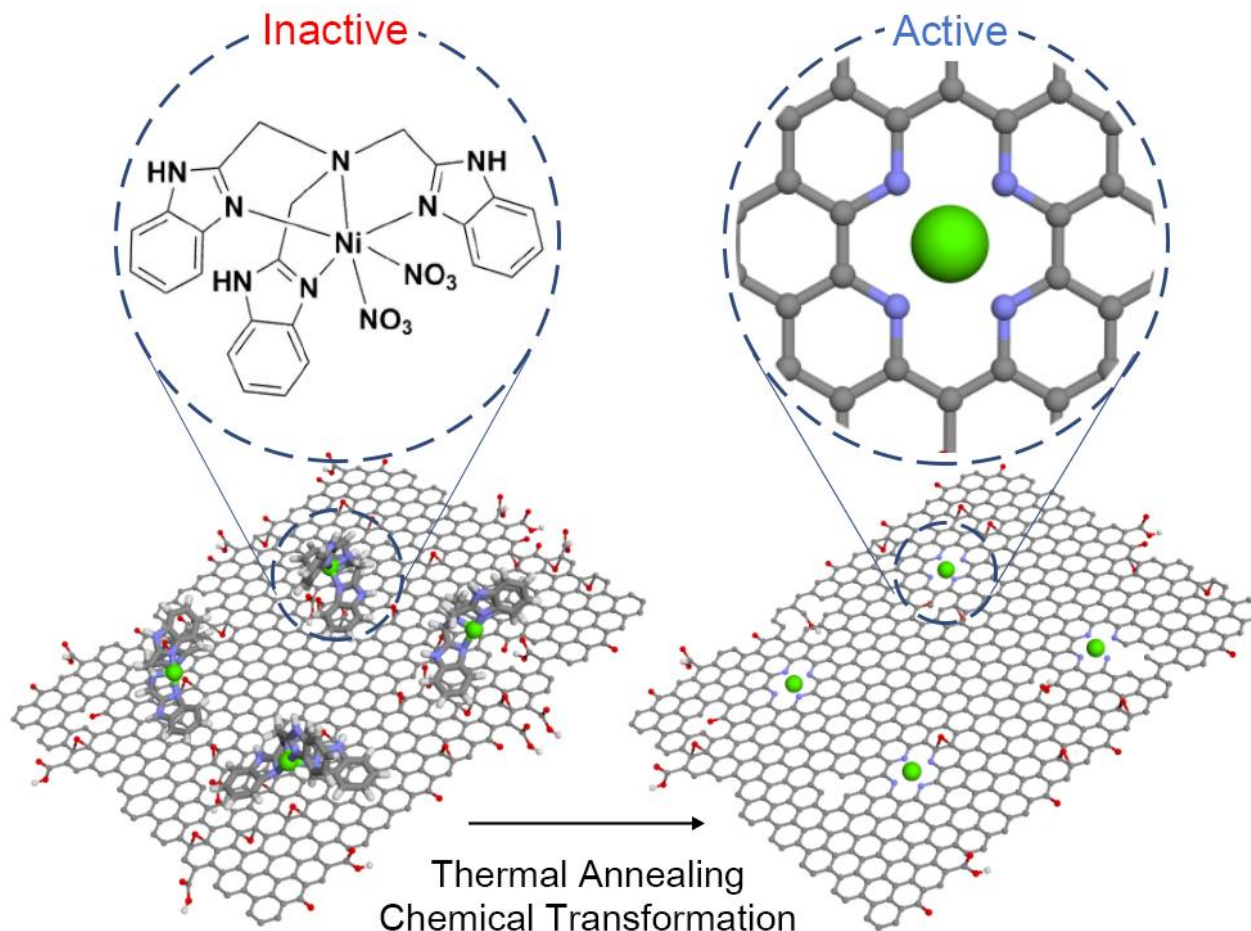
Ligand assisted metal doping over graphene oxide

TEM analysis

Ni(NTB) annealed _without GO sheets_

Ni(NTB) annealed _with GO sheets_
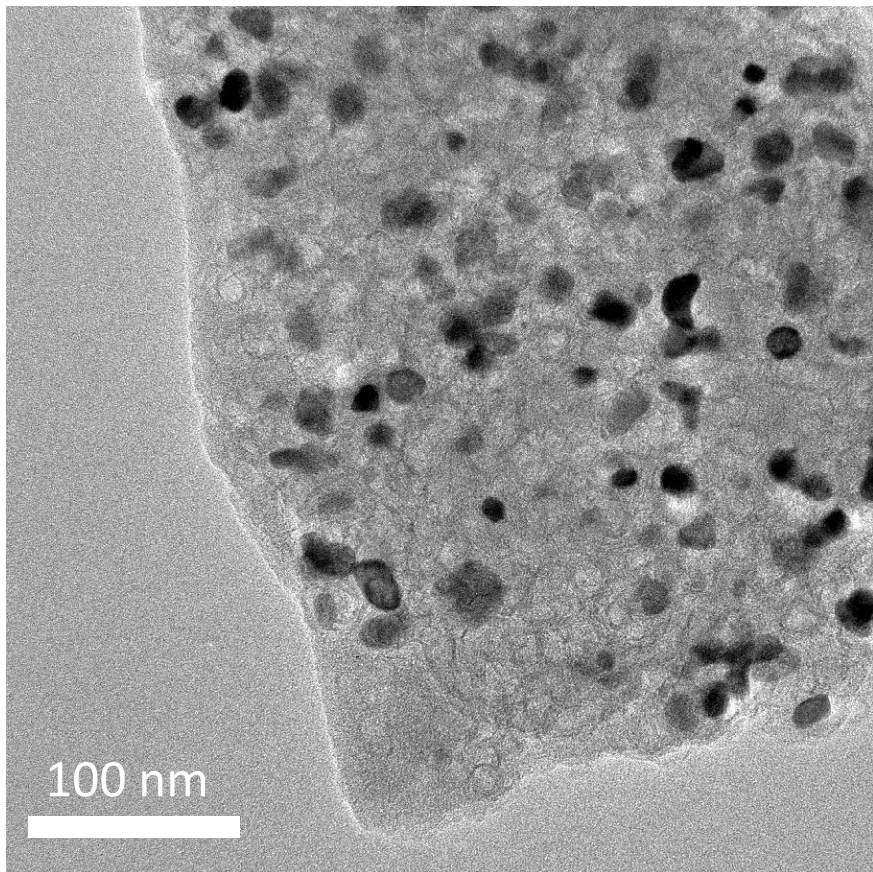
Agglomeration of Ni atoms
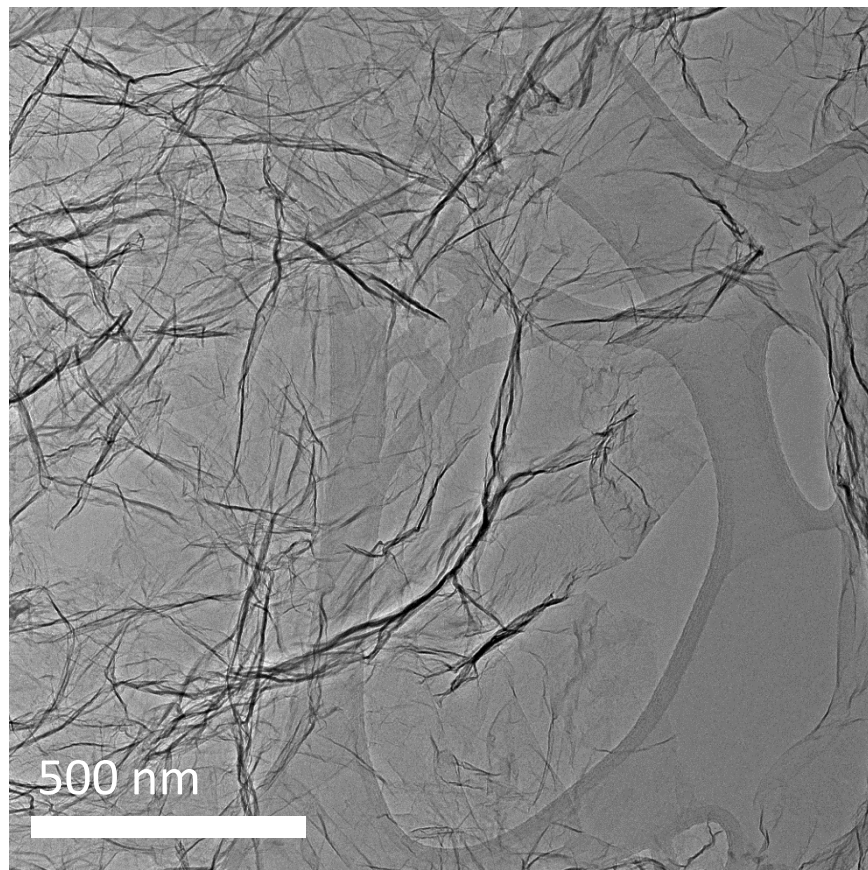
Prevented Ni atom agglomeration

Single-Atom Metal Active Sites on Graphene Oxide
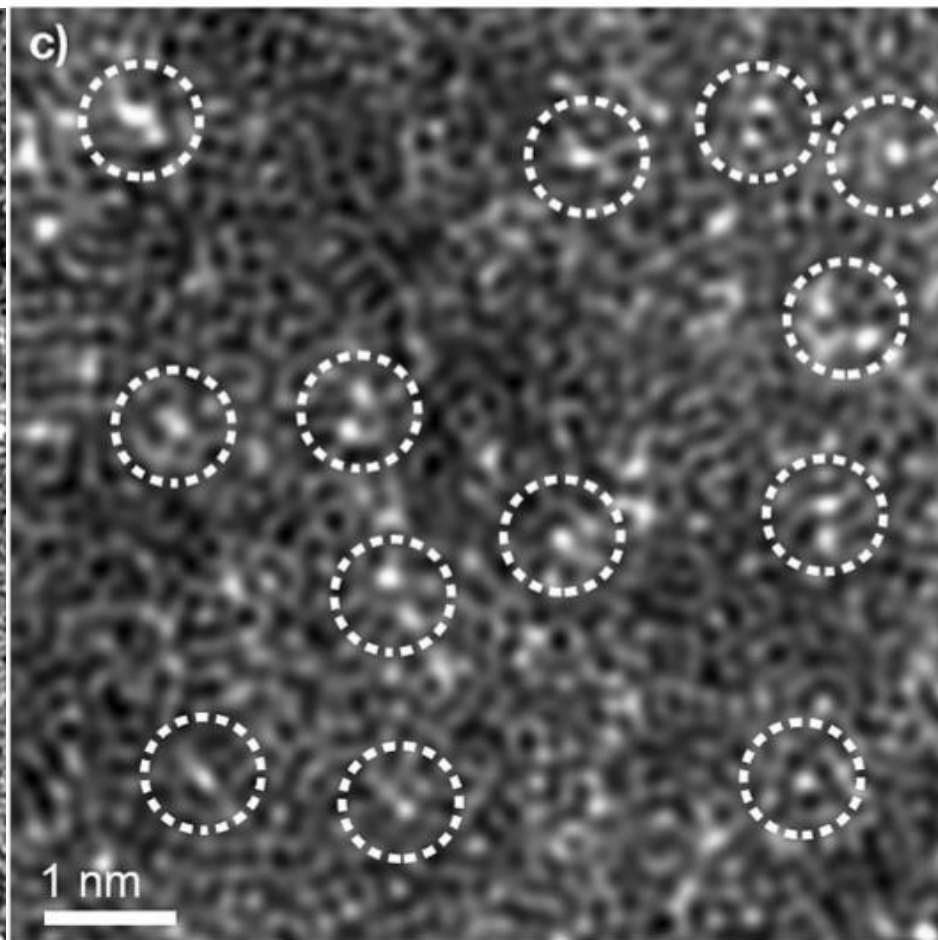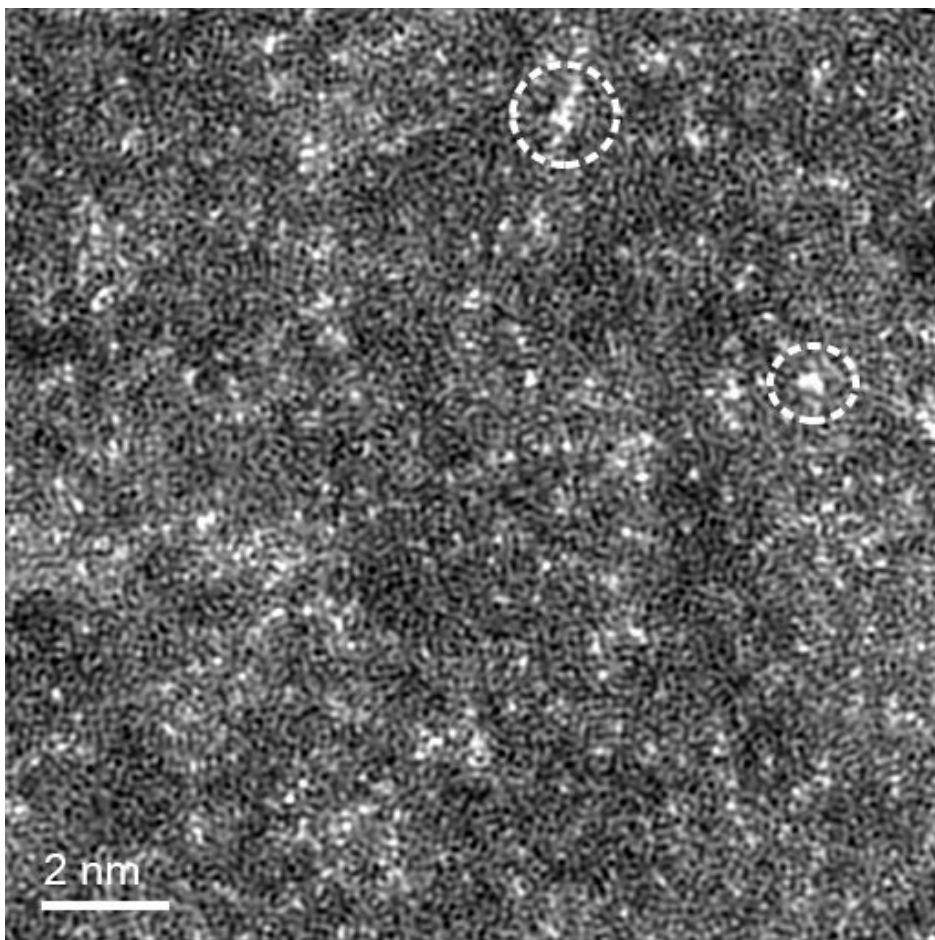
Uniform dispersion of Ni atoms over N-doped graphene oxide sheets

Chemical Structure by X-ray spectroscopy
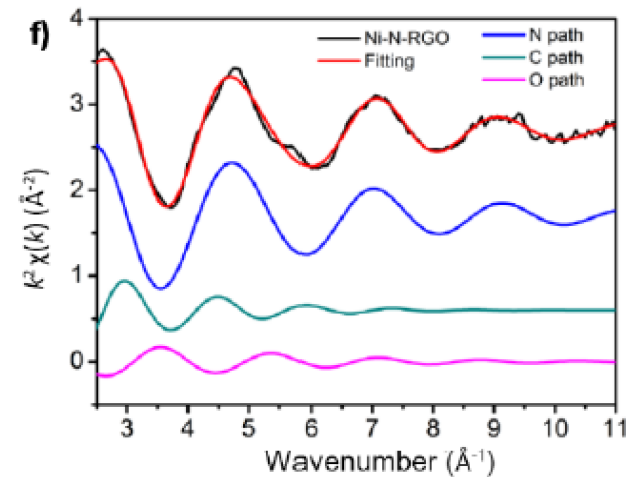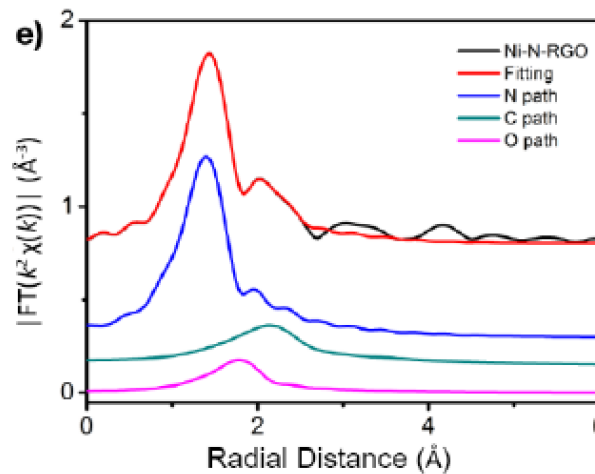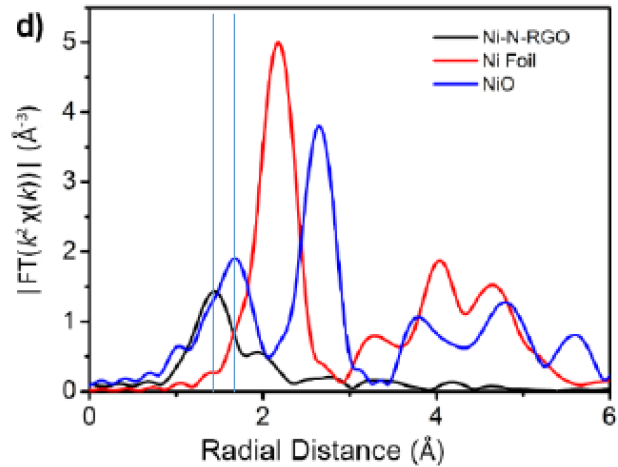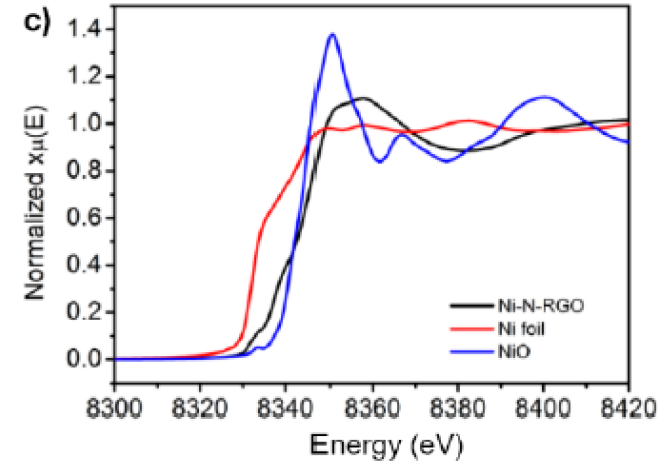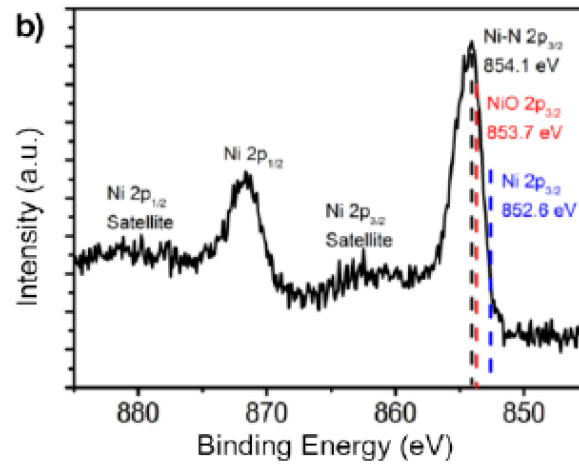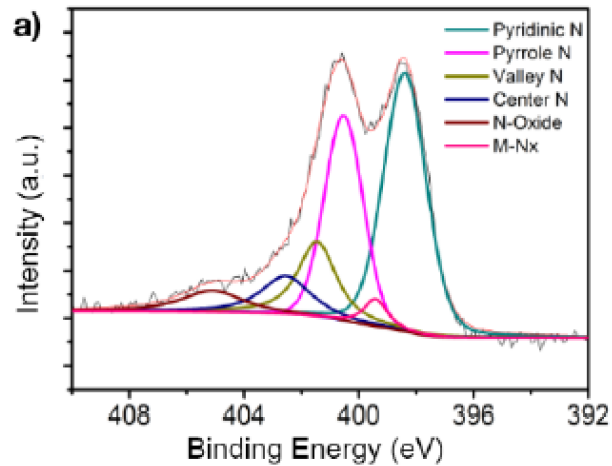
Metal- N4 moieties like metalloporphyrins or metallophthalocyanines

Ni-N₄C₄
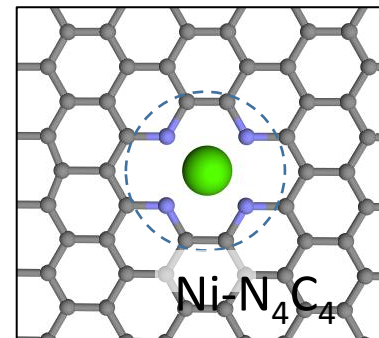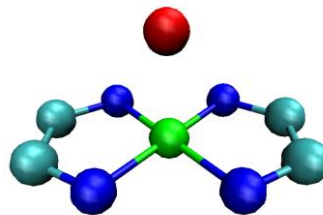
Ligand assisted Metal Doping over graphene oxide

Electrochemical activity of Ni-N-RGO

Linear sweep voltammetry
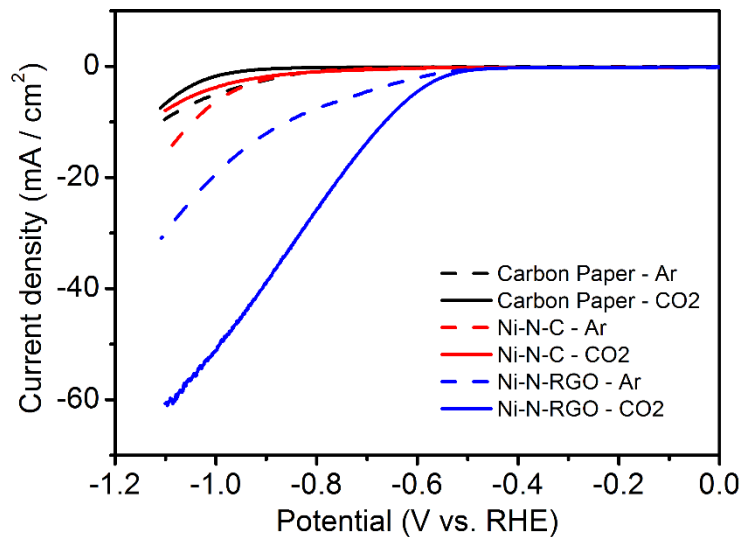
Faradaic efficiency
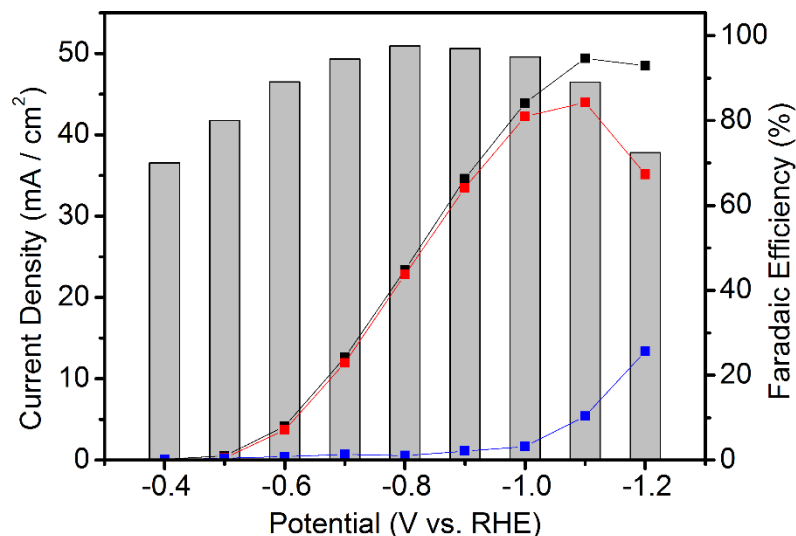
Tafel analysis
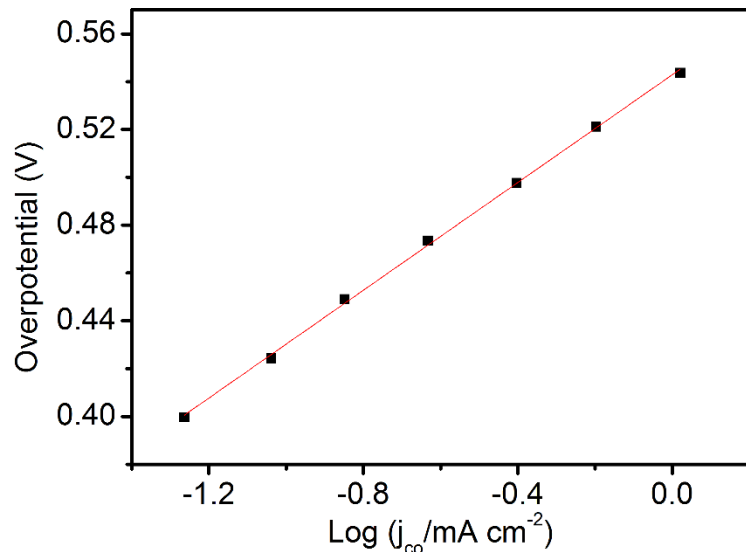
Dependence of current density on pH
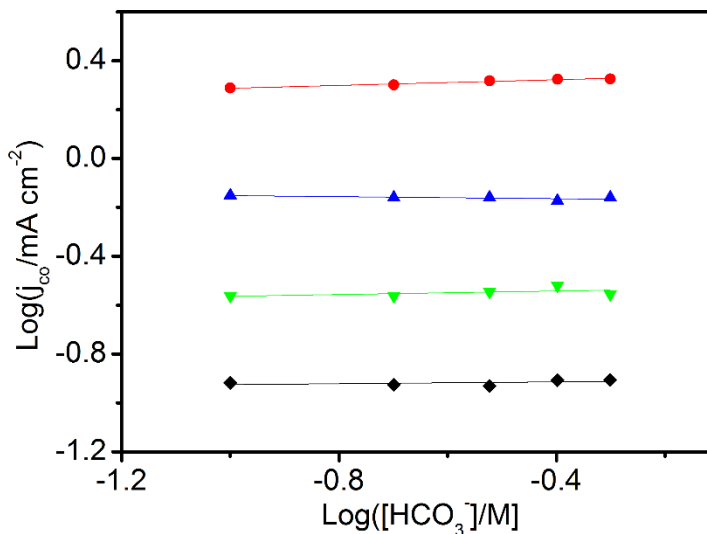
Ligand assisted Metal Doping over graphene oxide

Proposed reaction mechanism of Ni-N-RGO
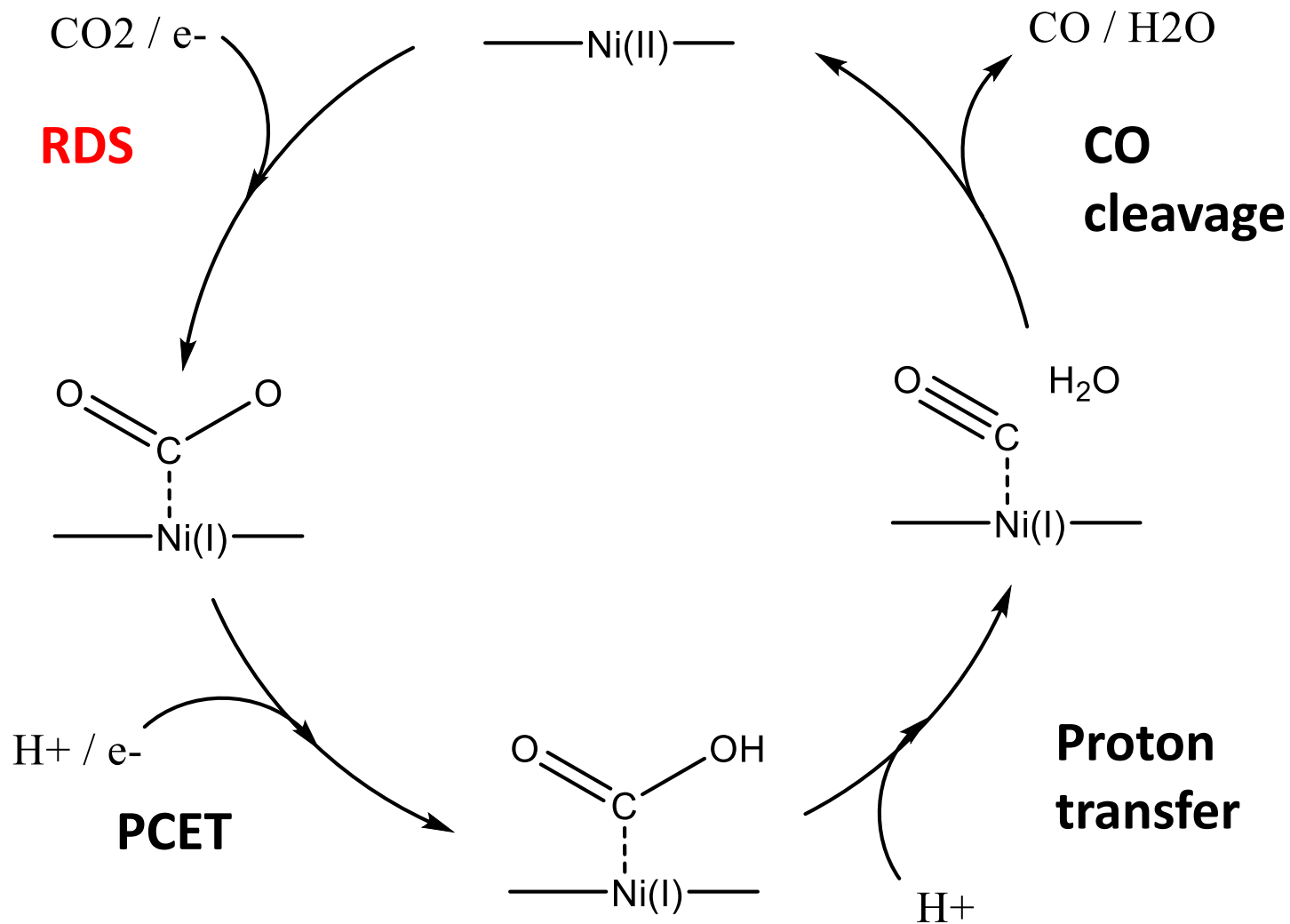
Ligand assisted Metal Doping over graphene oxide

Metal NTB carbonized with graphene oxide
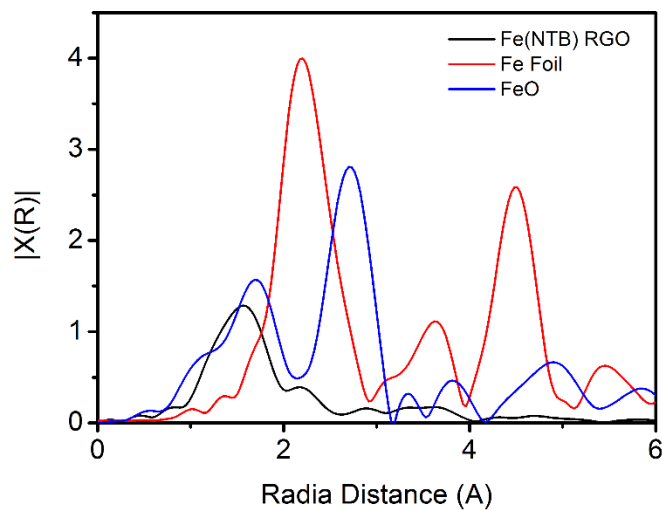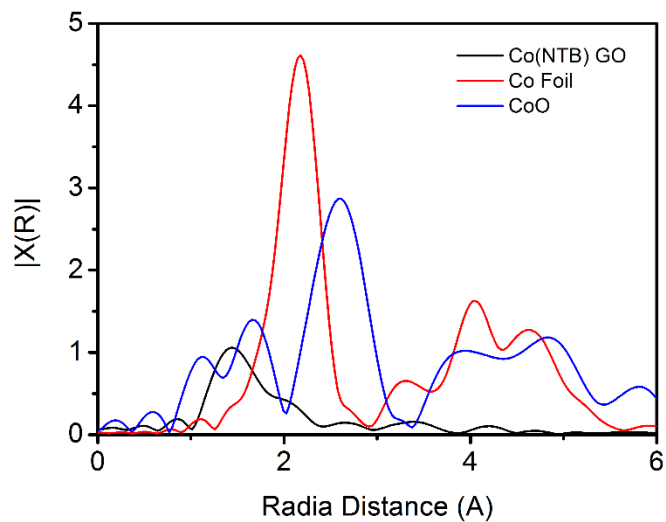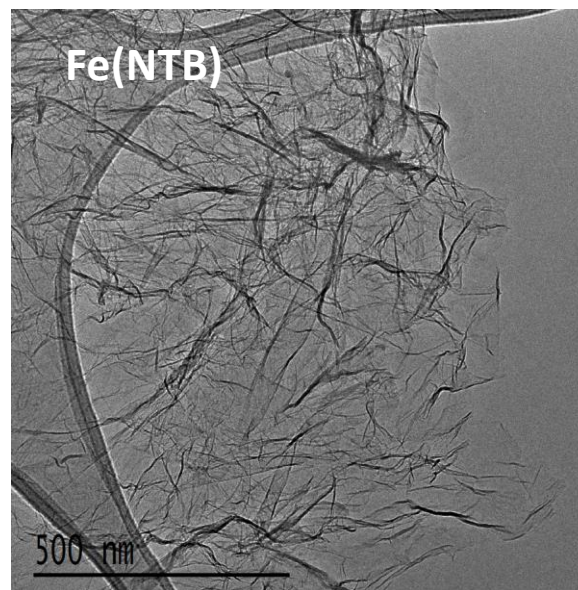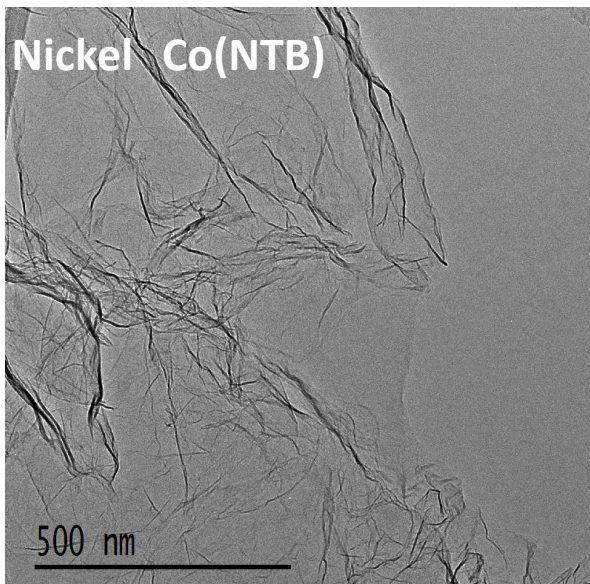
Ligand assisted Metal Doping over graphene oxide

Understanding selectivity of catalyst from DFT calculations

Ni-N-RGO
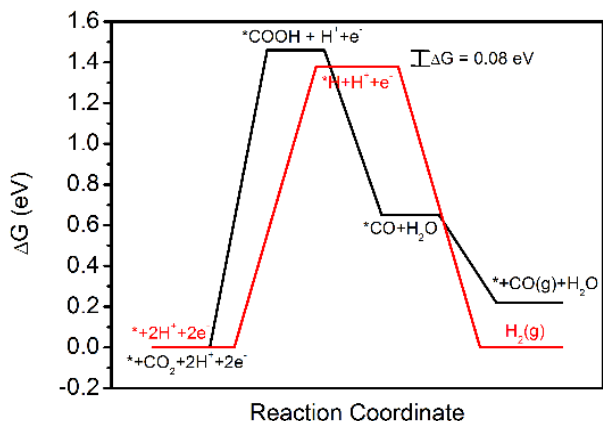
Fe-N-RGO
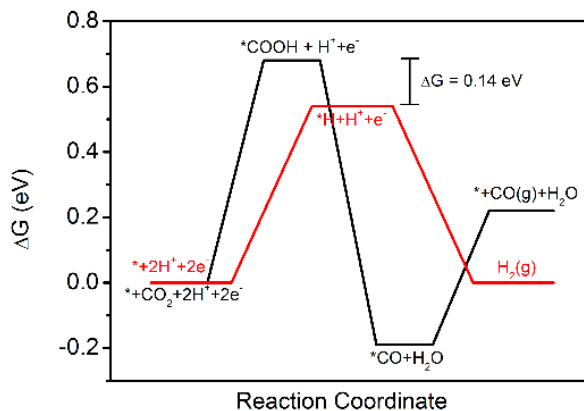
Co-N-RGO
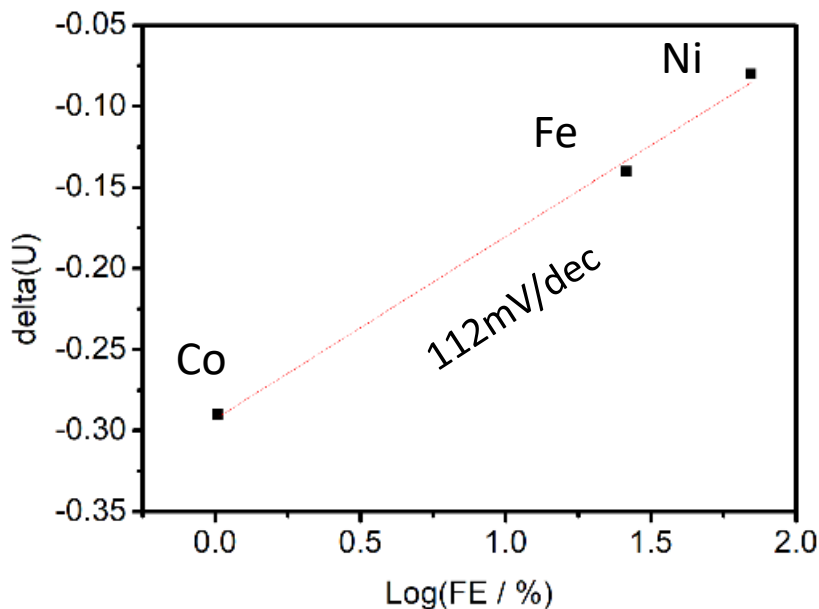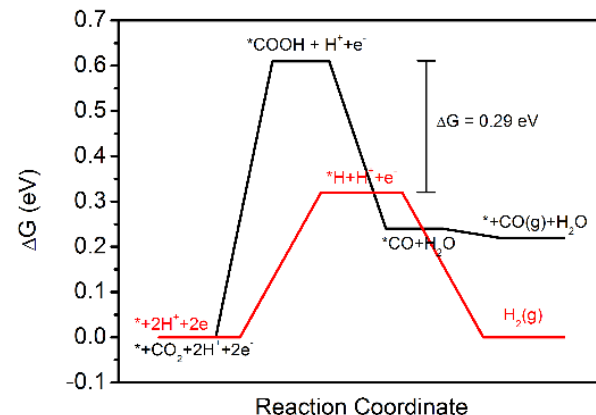
$$\frac{i_{co}}{i_{H_2}} = \frac{i_{0(CO)}\left(\exp\left[\frac{-\alpha_{CO}zF\eta_{CO}}{RT}\right]\right)}{i_{0(H_2)}\left(\exp\left[\frac{-\alpha_{H2}zF\eta_{H_2}}{RT}\right]\right)}$$

$$\log\left(\frac{j_{co}}{j_{H_2}}\right) = \frac{\alpha e}{kT}\left(U_{L(CO)} - U_{L(H2)}\right) + K$$

$$\frac{kT}{e\alpha} = \text{Tafel slope}$$

Ionic liquid derived Ni doped N Carbon for electrochemical CO production from CO_2

without silica supports

with silica supports

XANES

A : 1s-3d transition (quadrupole allowed transition)

B : 1s-4p_z transition (square planar M-N4)

C : 1s-4$p_{x,y}$ transition

D : Multiple scattering processes

800°C
900°C
1000°C
NiO
Ni

EXAFS

800°C
900°C
1000°C
NiO
Ni

Ar
CO_2

Ar
CO_2

Single scattering　　**Multiple scattering**
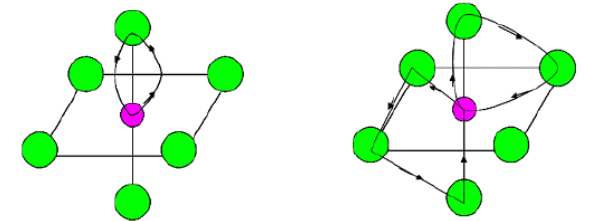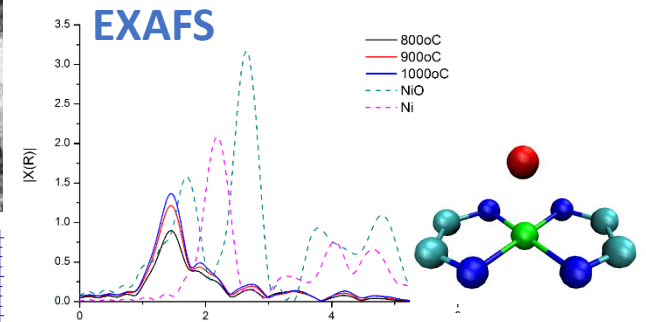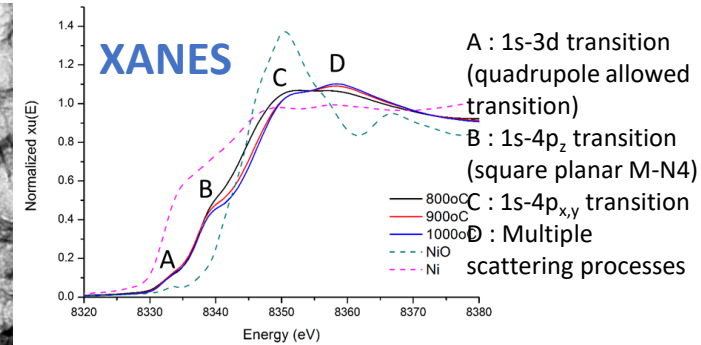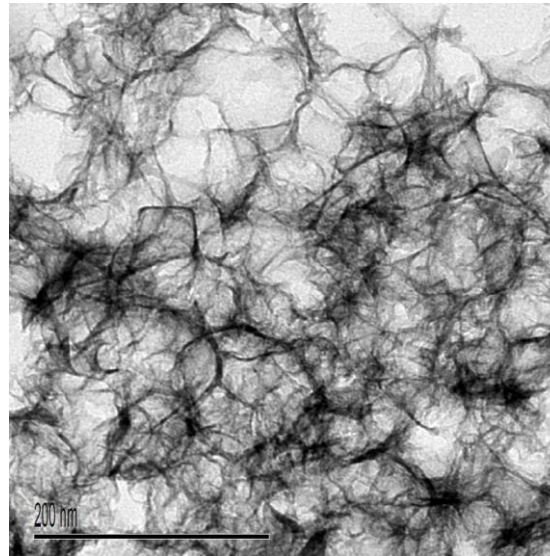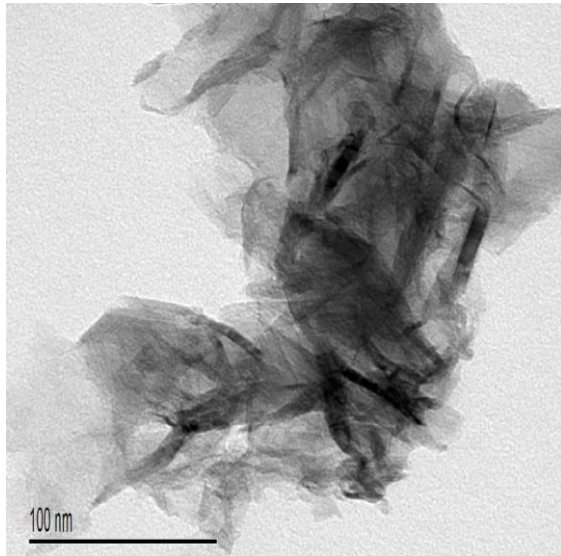
As the annealing temperature increases, Ni coordination structure becomes more symmetric.
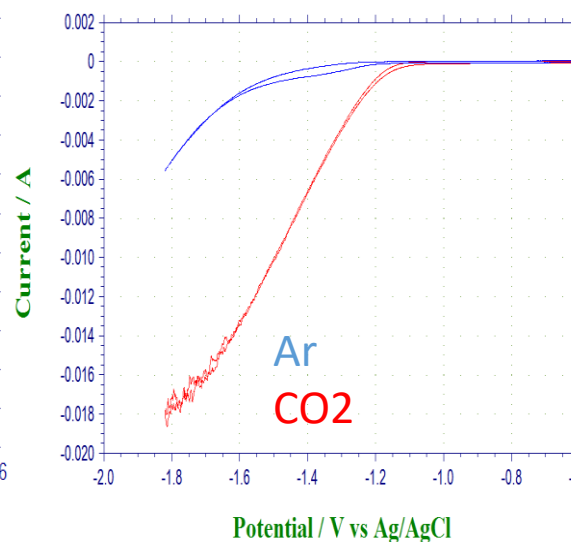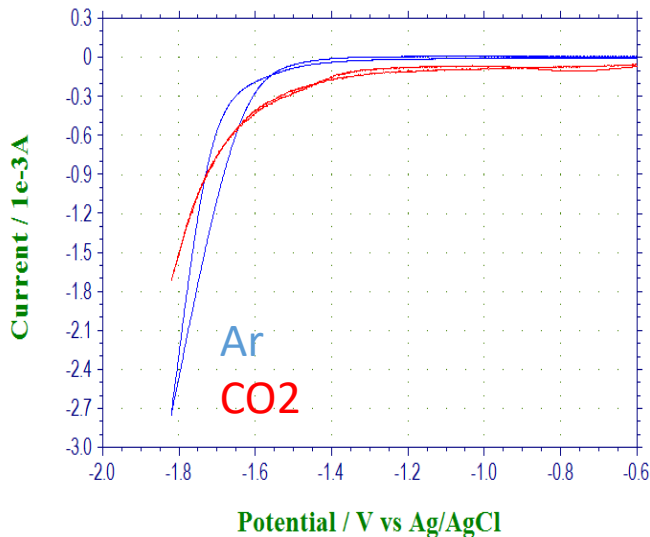
Ni-C₃N₄ Coated MWCNT for CO₂ Reduction

Oxidized MWCNT → Freeze drying With DCDA and NiCl₂ → Thermal annealing at 550°C → Etching excess nickel with HCl

Fit to Ni-N4C2

Bond length
Ni-N : 1.9 A
Ni-C : 2.15 A

EXAFS can be fitted with Nickel coordination number 4
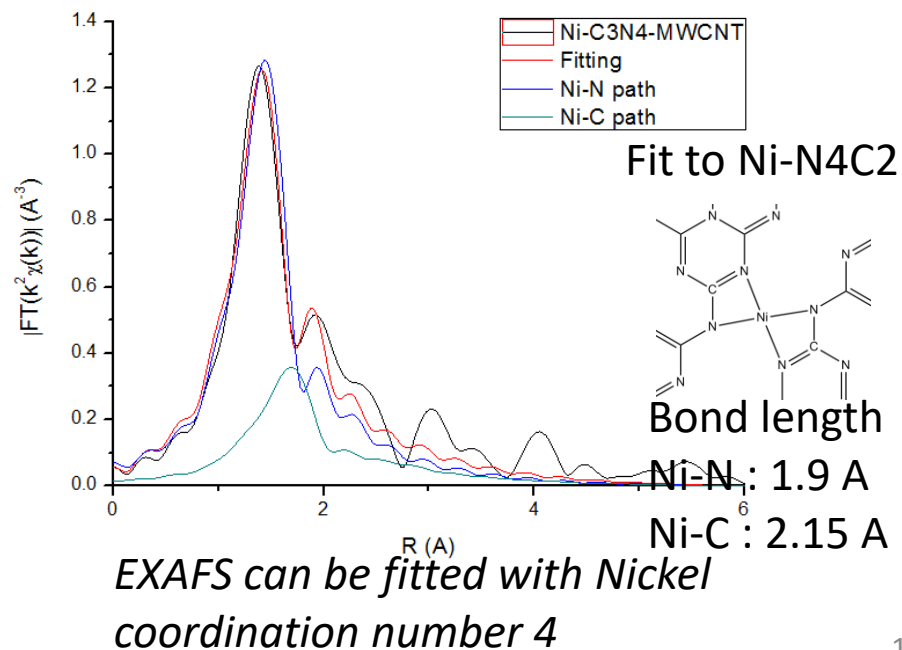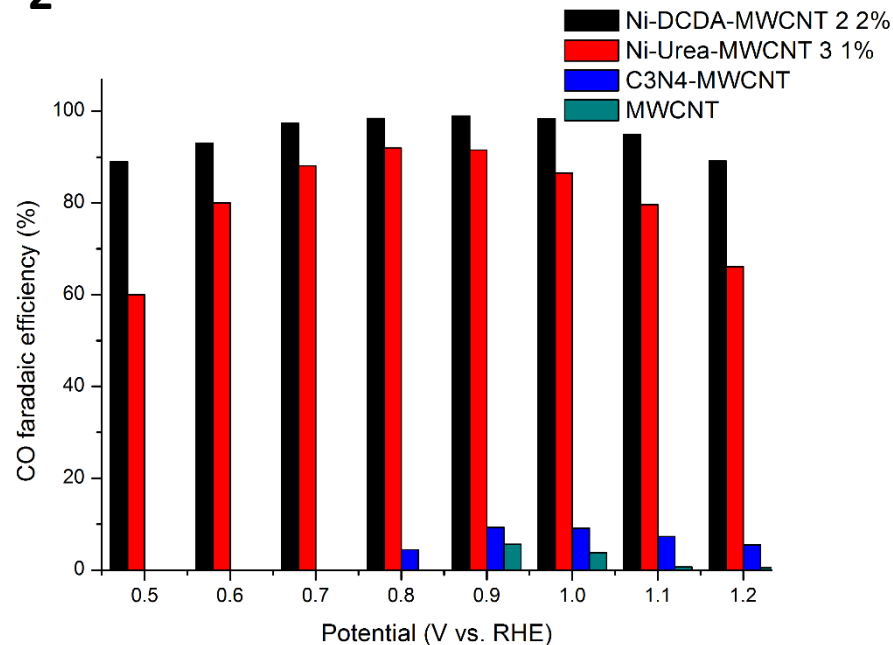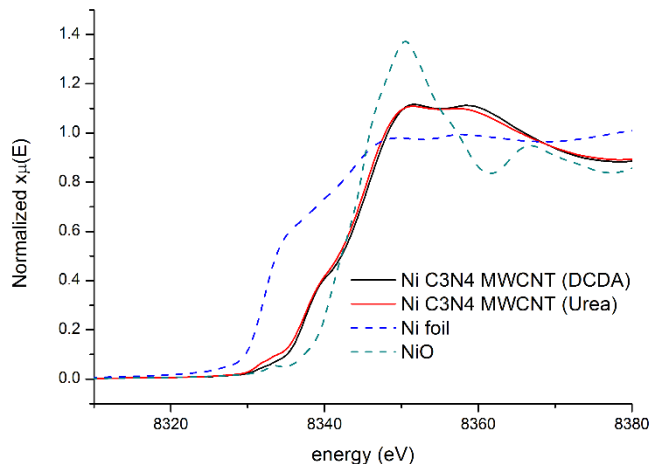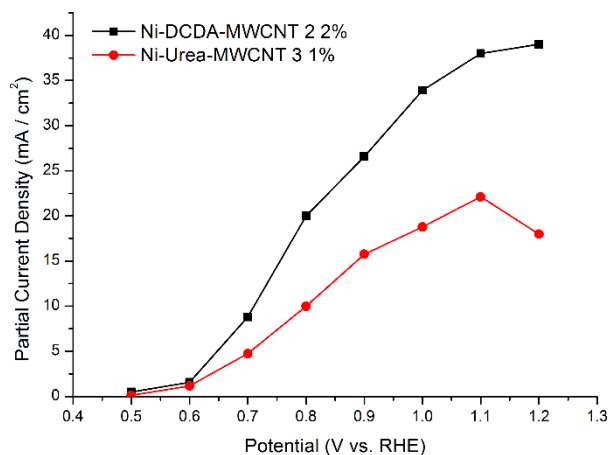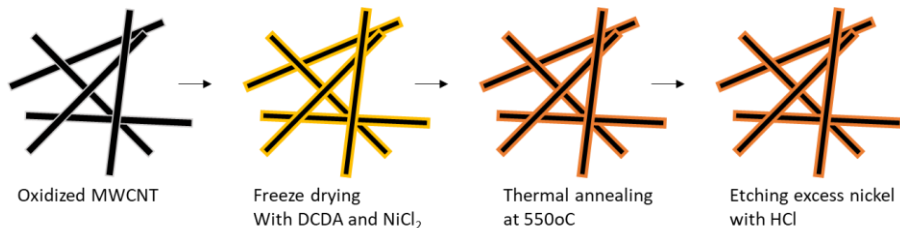
Achieving highly efficient CO2 to CO electroreduction exceeding 300 mA cm^{-2} with single-atom nickel electrocatalysts

Ni-SA-NC for CO$_2$RR

Synthesis of single atom nickel and nitrogen doped three-dimensional porous carbon electrocatalysts (Ni-SA-NCs).
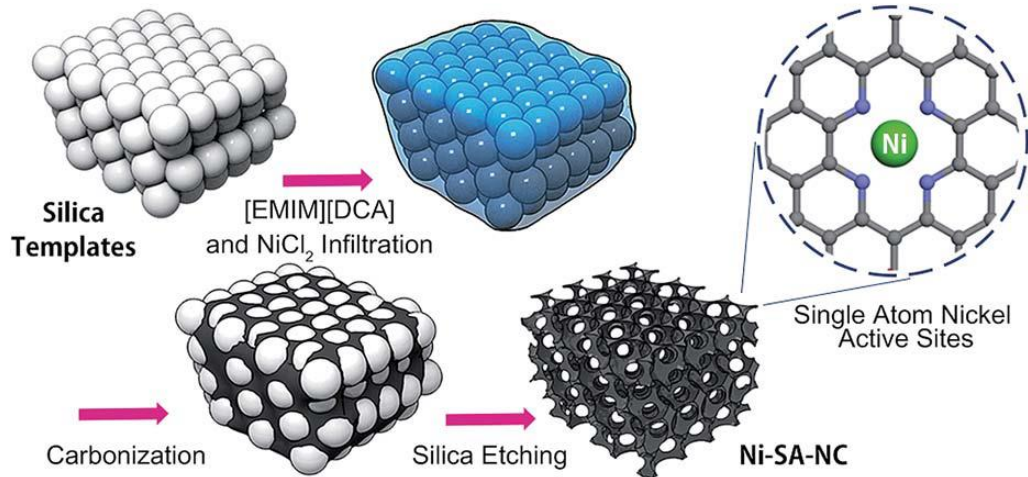
- Nitrogen coordinated single atom nickel sites were formed on the carbon surfaces as active sites for CO$_2$RR.

- A three-dimensional structure was adopted to increase the surface of the catalyst, thus enhancing the efficiency of the CO$_2$RR

FE-SEM, TEM, EDX mapping, and HAADF STEM images of Ni-SA-NCs.
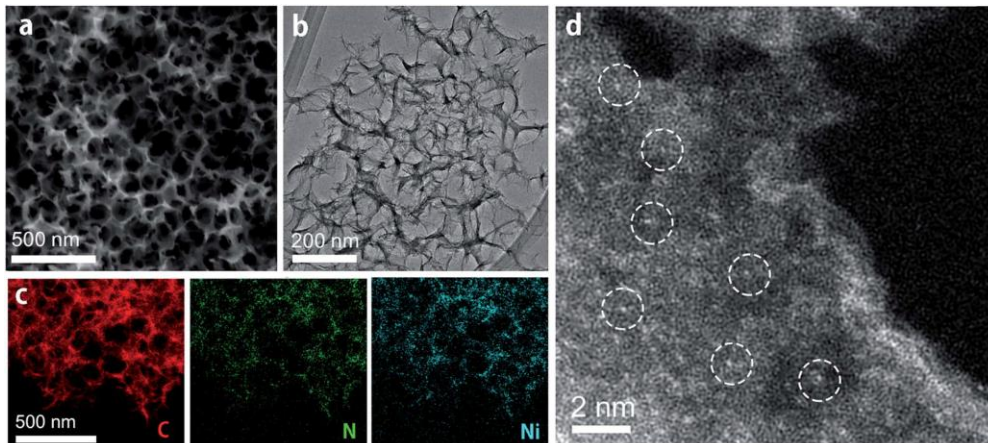
- Feld-emission scanning electron microscope (FE-SEM) and transmission electron microscopy (TEM) analysis of Ni-SA-NCs demonstrated a three-dimensional structure.

- Energy-dispersive X-ray spectroscopy (EDS) elemental mapping and high-angle annular dark field scanning transmission electron microscopy (HAADF-STEM) showed uniform dispersion of nickel atoms over the catalysts.

Ni-SA-NC for CO₂RR

XPS, RAMAN, XANES, and EXAFS of Ni-SA-NCs.
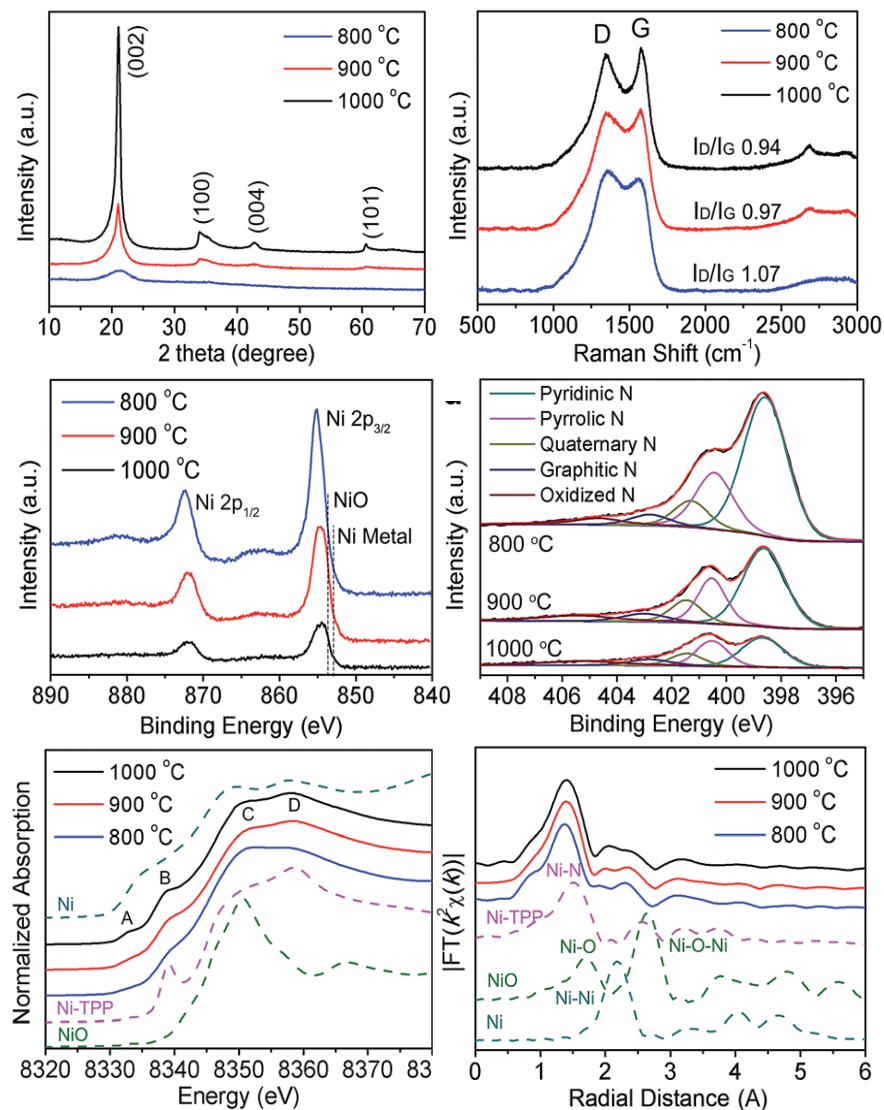
- X-ray diffraction (XRD) analysis indicated absence of peaks related to nickel materials suggests efficient removal of nickel agglomerates on Ni-SA-NCs.

- Raman spectroscopy showed that the carbonization temperature increases resulting the value of I_D/I_G for Ni-SA-NC decreases, and thus the number of defects in the Ni-SA-NCs is decreased.

- X-ray photoelectron spectroscopy (XPS) demonstrated that nitrogen and nickel were successfully doped on the carbon surfaces with the ionic characteristic of nickel atoms and various nitrogen defects.

- The Ni K-edge X-ray absorption near edge structure (XANES) their absorption edges are very close to those of nickel porphyrin (Ni-TPP) with a nickel valence state of 2+.

- X-ray absorption fine structure (EXAFS) analysis Ni-SA-NCs exhibit only one major peak around 1.42Å which can be assigned to a Ni–N pair.

Ni-SA-NC for CO_2RR

Scheme and DFT calculation of each coordination site

a — NiN4, NiN3V, NiN2V2, NiN3 coordination structures

b — ΔG (eV) vs Reaction Coordinate; *COOH + H$^+$+e$^-$; *CO+H$_2$O; *+CO(g)+H$_2$O; *+CO$_2$+2H$^+$+2e$^-$; legend: NiN4, NiN3V, NiN2V2, NiN3

c — ΔG (eV) vs Reaction Coordinate; *H+H$^+$+e$^-$; *+2H$^+$+2e$^-$; *+H$_2$(g); legend: NiN4, NiN3V, NiN2V2, NiN3
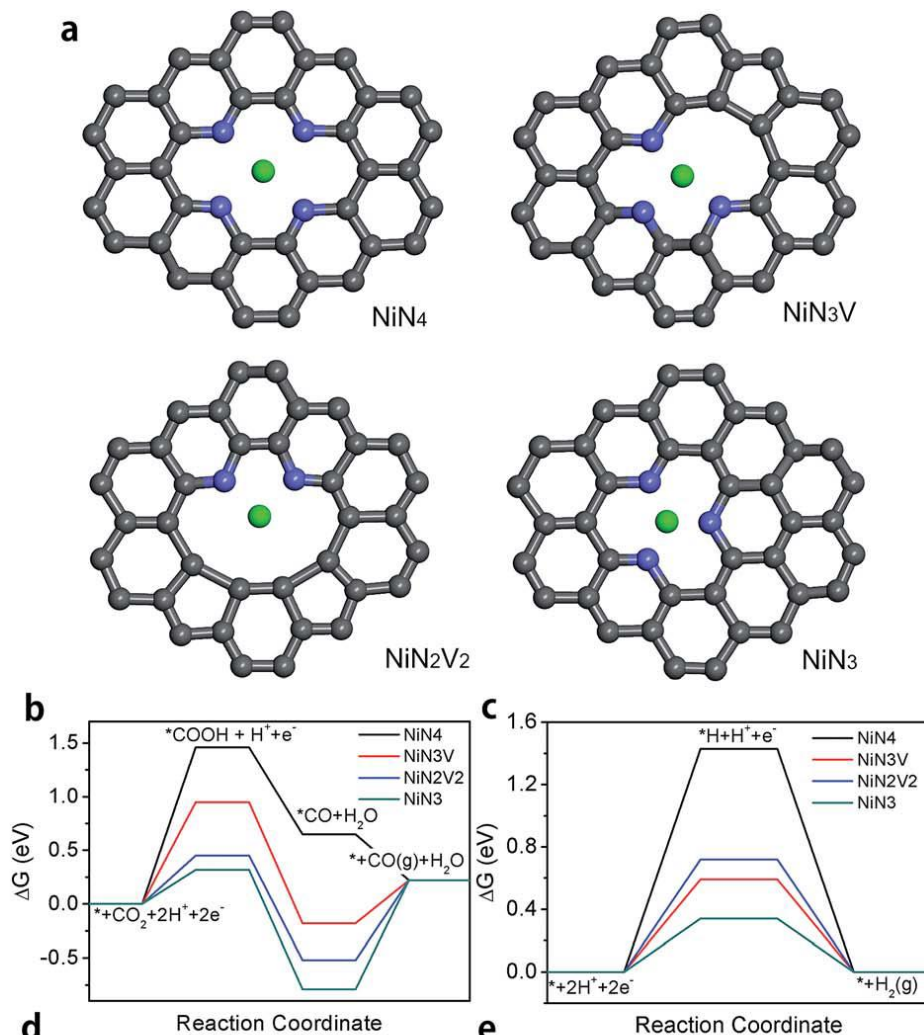
- Four different nickel coordination structures were considered, NiN_4, NiN_3V, NiN_2V_2, and NiN_3.

- The potential for COOH* formation is the limiting potential for CO_2RR. NiN_3, NiN_3V, and NiN_2V_2 show lower free energies of COOH* formation than NiN_4 suggesting that CO_2 can interact more easily with these low coordination number nickel sites to form the COOH* intermediate at a lower applied potential.

- But, the limiting potential for the competitive hydrogen evolution reaction also decreases with these less coordinated nickel sites which can result in dominant hydrogen production.

- From the DFT calculation, the fully nitrogen coordinated Ni–N_4 active sites on the graphitic lattices facilitate highly selective CO production.

Ni-SA-NC for CO$_2$RR

LSV, FE, and Tafel analysis of Ni-SA-NC

MEA cell with EC analysis
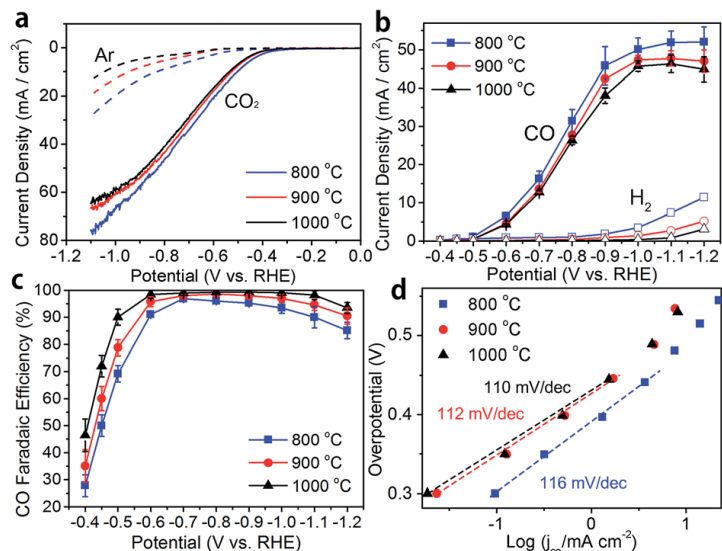
- the CO$_2$ was purged into the electrolyte, the current density increased significantly, exceeding 50 mA cm^{-2} at 1.0 V vs. RHE.

- Ni-SA-NC prepared at 1000 C shows a maximum faradaic efficiency for CO$_2$ reduction exceeding 99%.

- Tafel slope was calculated as 110 mV dec^{-1}. This value is close to 118 mV dec^{-1}, suggesting that one electron transfer is involved in the rate-determining step (RDS).

- The CO$_2$ reduction efficiency was further improved by introducing the membraned electrode assembly (MEA) cell.

- The direct supply of CO$_2$ to the surface of the catalysts significantly enhances the limited mass transfer of CO$_2$ in the aqueous electrolytes, and a high CO production rate of over 300 mA cm^{-2} can be achieved.

Ni and N co-doped Hollow Carbon Sphere for CO$_2$RR

Ni, N-Hollow Carbon Sphere for CO$_2$RR

Introduction

Characteristics of Single Atom Catalysts
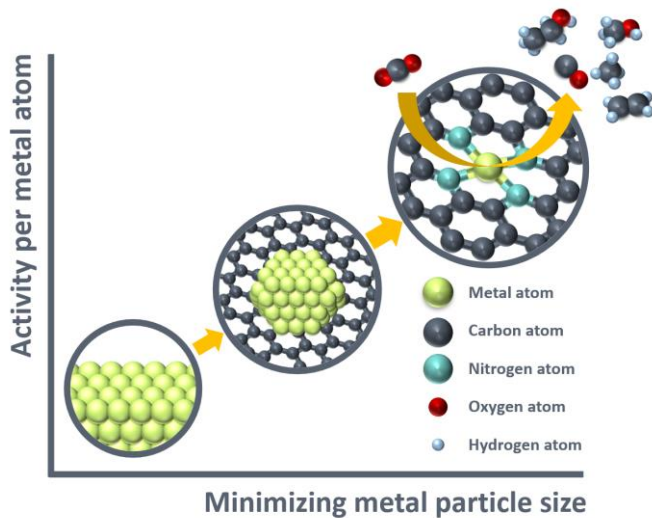
SACs utilize inexpensive transition metals and maximize atomic utilization to decrease the cost of synthesis.

The d-bands of transition metals of SACs have valence electrons that are close to the Fermi level overcoming the intrinsic activation barriers.

Particularly, the binding strength between the metal atom and coordinated N atoms is strong enough to achieve high stability due to the 2p orbitals of nitrogen hybridizing with the d orbitals of the transition metal atom.

Tetramer model of melanin
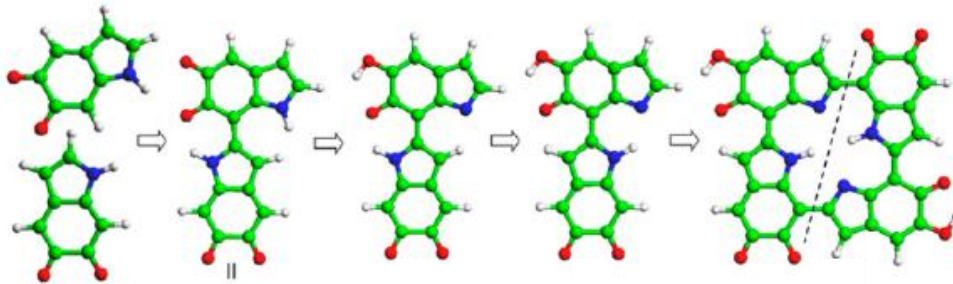
Melanin can storage, release, exchange the metal ion.

Tetramer model of melanin have four-nitrogen atoms anchoring metal ions.

Sheng Meng et al., Biophys. J. (2008)

Ni, N-Hollow Carbon Sphere for CO$_2$RR

Scheme of the Ni-N-HCS

Silica → Ni-PDA@Silica → Ni-C@Silica → Ni, N-HCS

Ni&PDA coating
pH = 8.5, Tris-HCl buffer solution at 25℃ for 24h

Carbonization
In N2 condition at 800℃ for 2h

Etching
5% HF aqueous Solution for 1 day
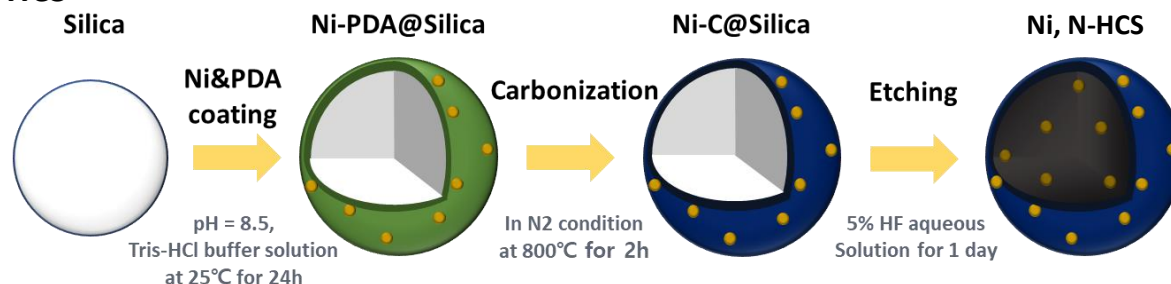
SEM images

Silica (SiO2) nanoparticles

250 nm
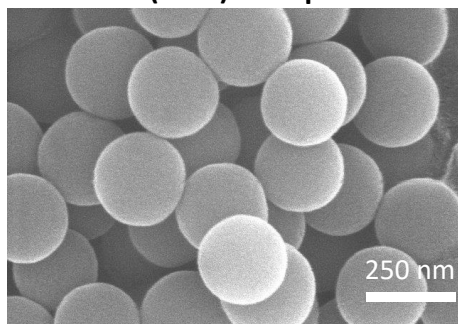
Ni and Polydopamine@SiO2

250 nm

- *Average size of particles of SiO2 ≒253.10nm*

Ni, N-C@SiO2

250 nm
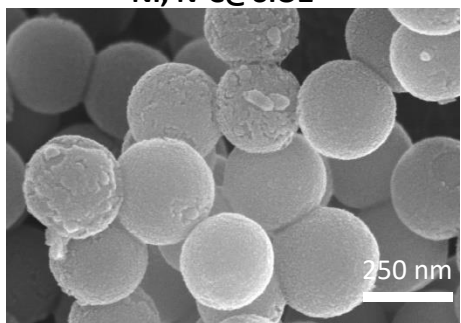
Ni, N-Hollow Carbon Sphere(HCS)

250 nm
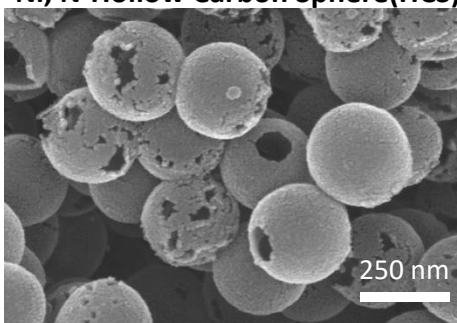
- *Average size of particles of N-N-HCS ≒278.2nm*

TEM and EDS images

Ni, N-HCS

50 nm

10 nm

100 nm

Ni-K — 100 nm

Ni-L — 100 nm

C — 100 nm

N — 100 nm

O — 100 nm
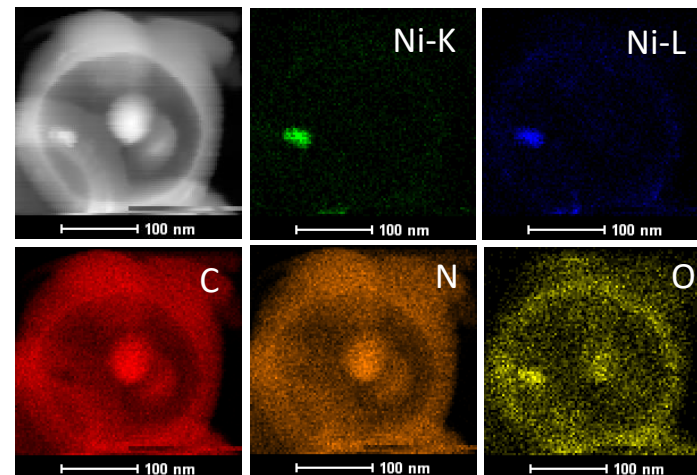
Ni, N-Hollow Carbon Sphere for CO_2RR

X-ray Diffraction (XRD)
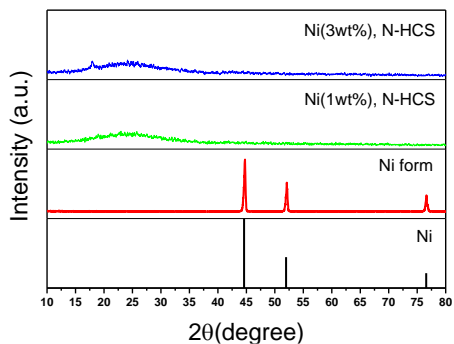
- XRD of Ni, N-HCS didn't show the Ni peaks.

  → indicating that Ni atoms are dispersed well

	C 1s (at. %)	N 1s (at. %)	Ni 2p (at. %)
Ni(3wt%), N-HSC	79.53	4.36	0.65
Ni(1wt%), N-HSC	83.83	4.6	0.71
HCS	88.86	8.44	N/V

X-ray photoelectron spectroscopy (XPS)

Ni(3wt%), N-HCS
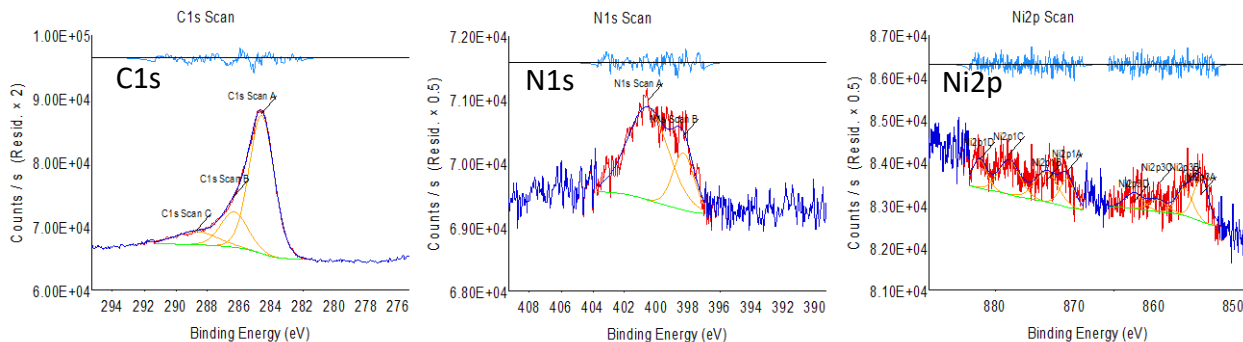
Ni(1wt%), N-HCS
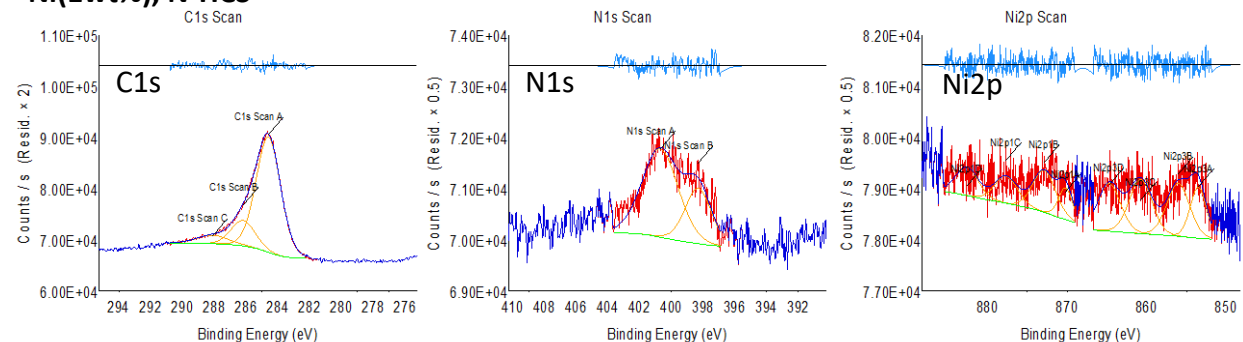
HCS without Ni precursor

Ag and N co-doped Carbon Quantum Dots for CO$_2$RR

Ag, N-Carbon Quantum Dots for CO$_2$RR

Introduction

Carbon Quantum Dots

Low cost

Easy surface passivation and functionalization

High chemical stability and inertness

High electrical conductivity

Good biocompatibility

Fluorescence properties

Application

Biosensing
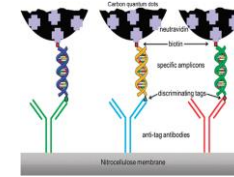
Chemical sensing
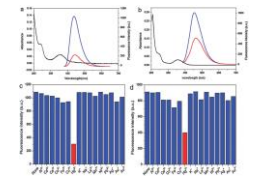
Bioimaging
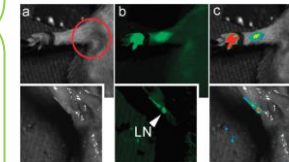
Nanomedicine
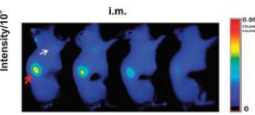
Electrocatalysis
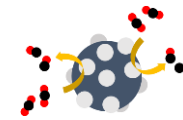
Photocatalysis

Scheme of the Ag, N-CQDs

Fumaronitrile (C$_4$H$_2$N$_2$)

AgNO$_3$

DI water

Teflon-lined autoclave

Hydrothermal reaction at 200℃, 15min

Filtration with PTFE membrane

Centrifugation

Freeze-drying
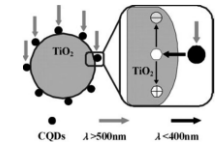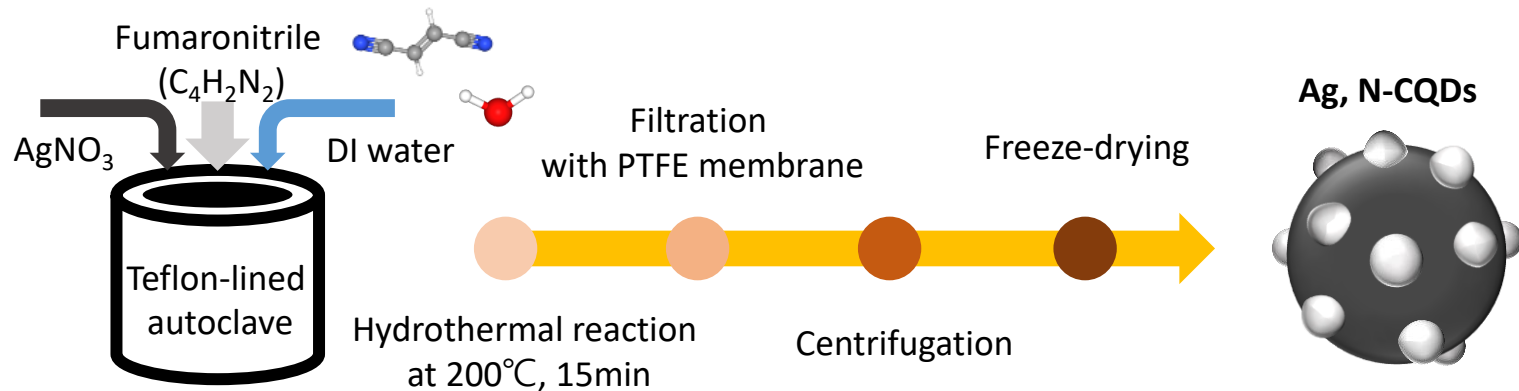
Ag, N-CQDs

Ag, N-Carbon Quantum Dots for CO$_2$RR

SEM of Ag, N-CQDs

TEM of Ag, N-CQDs

2.392Å

2. 13Å

2.422Å
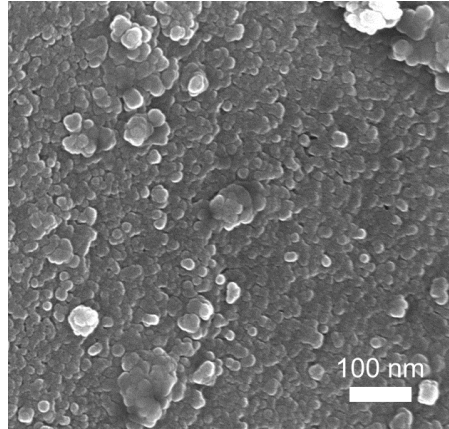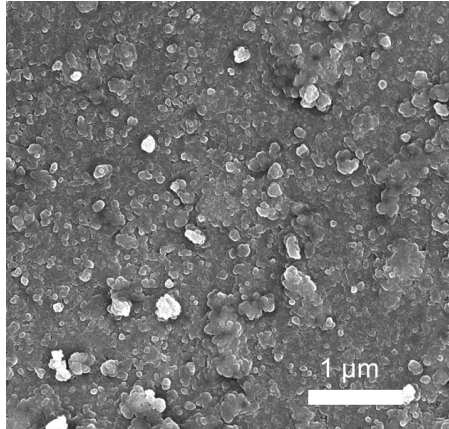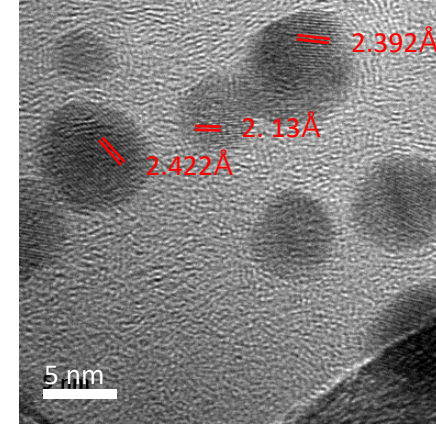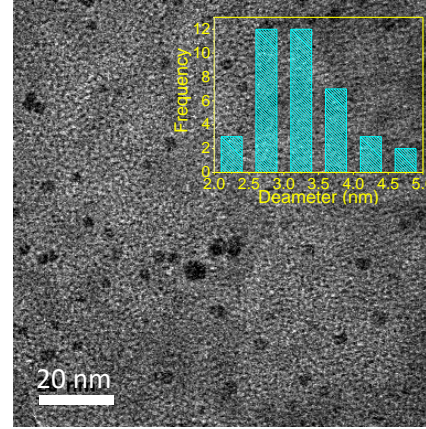
SEM of Ag nanoparticles for reference
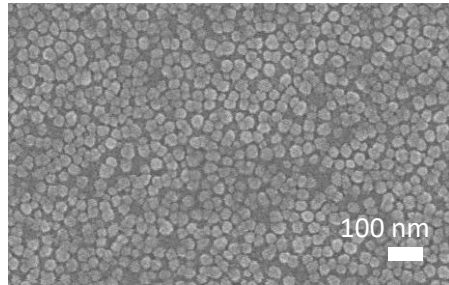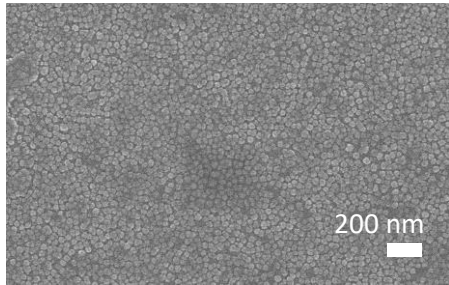
- All the obtained CQD were spherical morphology with an average diameter of 3.3 nm.

- Bright particle showed 2.1Å of d-space
  → indicating CQD
- Dark particle showed 2.4Å of d-space
  → indicating Ag

Reference number : 96-151-2488

Ag, N-Carbon Quantum Dots for CO$_2$RR

XPS of the Ag-CQD

FT-IR and UV-Vis of the Ag-CQD
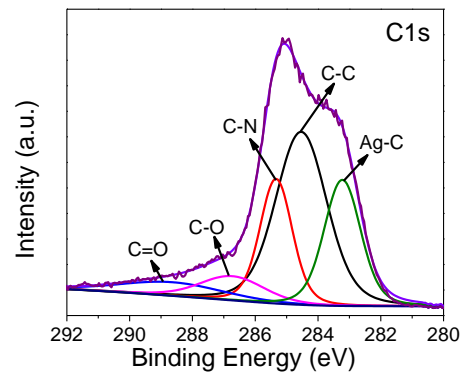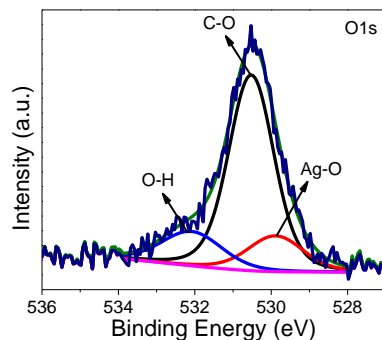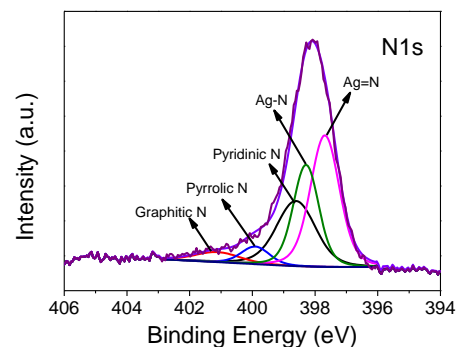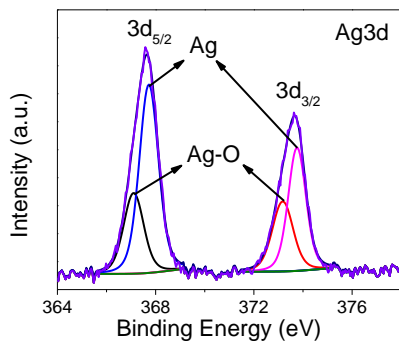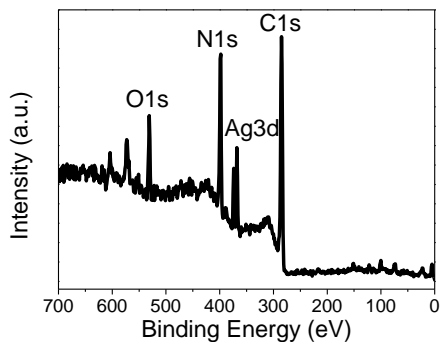
Name	Peak BE	Atomic %
C1s	284.94	65.57
N1s	398.52	24.49
Ag3d	368.02	1.44
O1s	531.12	8.5
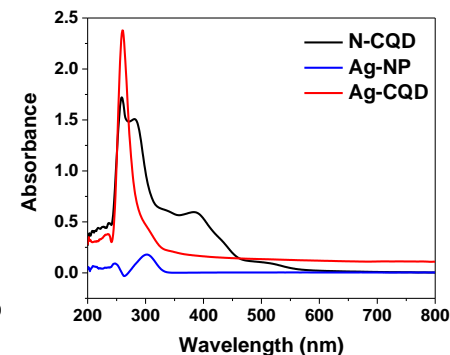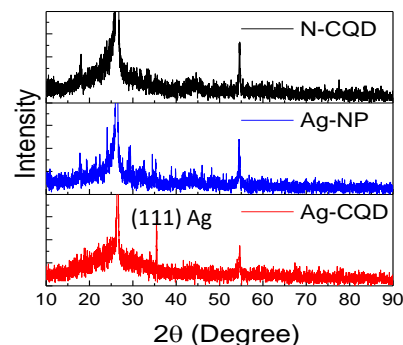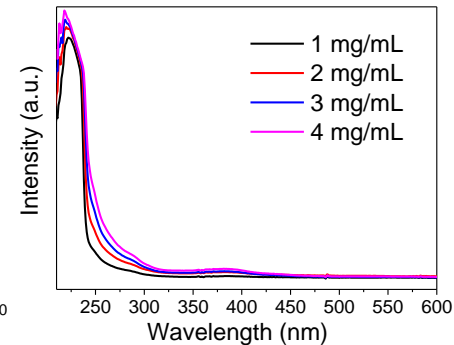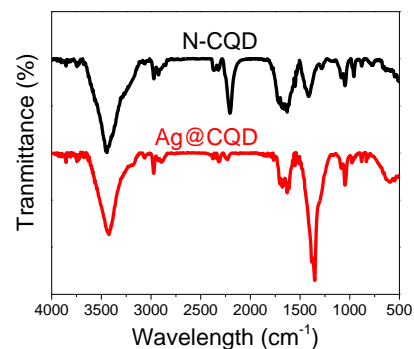
- XRD of N-CQD, Ag-NP, and Ag-CQD showing (111) index plane of Ag metal in Ag-CQD.

- UV-vis absorption spectra of N-CQD, Ag-NP, and Ag-CQD (10mg/ml)

- The XPS data of Ag-CQD showed Ag, O, N, and C peak with virous bonding energy.
- The Ag 3d peak elucidated that Ag existed.
- The N 1s peak showed that N atoms are coordinated with Ag such as Ag-N and Ag=N bonding.
- The XPS demonstrated the amount of Ag (1.44 at. %).

Ag, N-Carbon Quantum Dots for CO$_2$RR

CO2 reduction reaction
(Three electrode system at 0.5M KHCO$_3$)
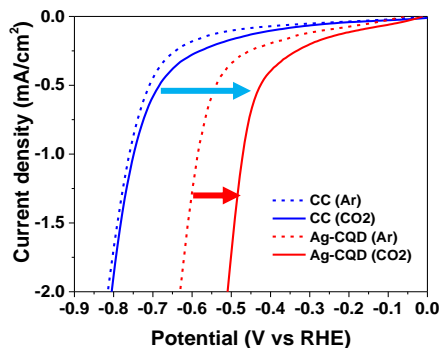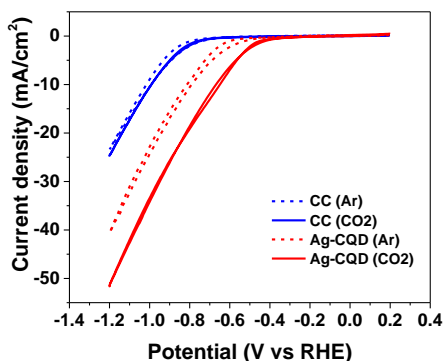
GC analysis for FE

- The redox peak is not observed in CV of CO2 reduction.
  → Indirectly indicating that Ag particle is absent.

- Onset potential (1mA/cm^2)

  Bare CC (Ar) : -0.764 (V vs RHE)
  Bare CC (CO2) : -0.749
  Ag-CQD (Ar) : -0.859
  Ag-CQD (CO2) : -0.472

Sample	Onset potential at 1 mA/cm^2 (V vs. RHE) at Ar condition	Onset potential at 1 mA/cm^2 (V vs. RHE) at CO2 condition
Bare CC	-0.764	-0.749
Ag-CQD/CC	-0.589	-0.472
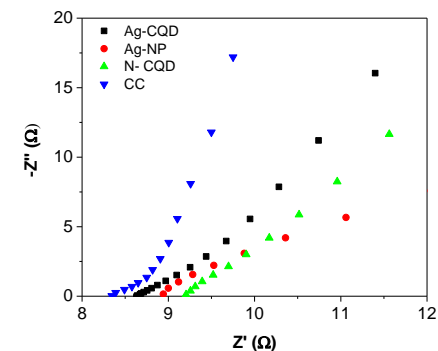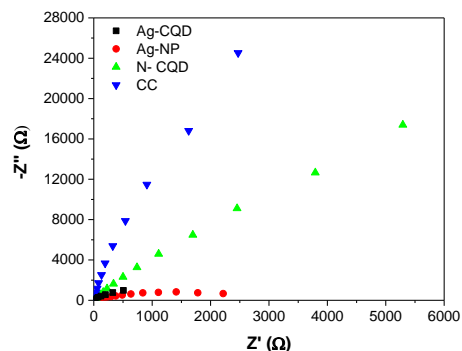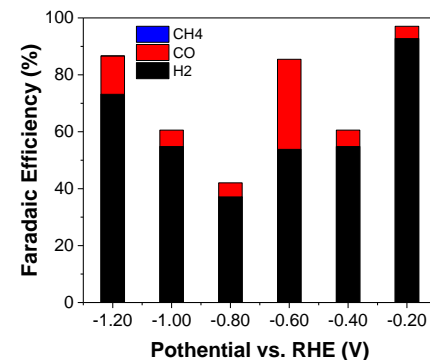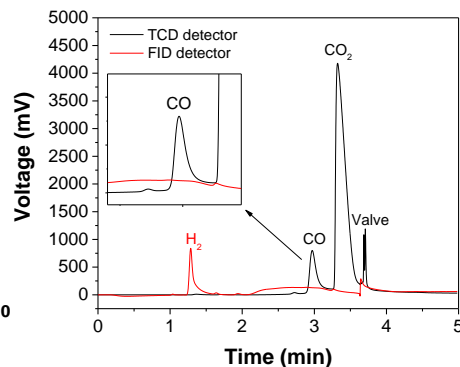
- Using Ag-CQD at CO$_2$ condition enhance the activity of the CO$_2$RR than bare carbon cloth (CC).

- Activity of the Ag-CQD at CO$_2$ condition is superior than Ar condition showing the supplied CO$_2$ accelerate the reaction.

- The product CO and CH$_4$ can be detected using gas chromatography and demonstrated.